Animal Study

Multivariate Pattern Analysis in Identifying Neuropathic Pain Following Brachial Plexus Avulsion Injury: A PET/CT Study

Ao-Lin Hou, MD[1], Jia-Jia Wu, MD, PhD[2], Xiang-Xin Xing, MD[3], Bei-Bei Huo, MD, PhD[3], Jun Shen, MD, PhD[4], Xu-Yun Hua, MD, PhD[1], Mou-Xiong Zheng, MD, PhD[1], and Jian-Guang Xu, MD, PhD[3,5]

From: [1]Department of Trauma and Orthopedics, Yueyang Hospital of Integrated Traditional Chinese and Western Medicine, Shanghai University of Traditional Chinese Medicine, Shanghai, China; [2]Departments of Rehabilitation Medicine, Yueyang Hospital of Integrated Traditional Chinese and Western Medicine, Shanghai University of Traditional Chinese Medicine, Shanghai, China; [3]School of Rehabilitation Science, Shanghai University of Traditional Chinese Medicine, Shanghai, China; [4]Department of Orthopedics, Guanghua Hospital of Integrative Chinese and Western Medicine, Shanghai, China; [5]Engineering Research Center of Traditional Chinese Medicine Intelligent Rehabilitation, Ministry of Education, Shanghai, China

Address Correspondence:
Jian-Guang Xu, MD, PhD
School of Rehabilitation Science, Shanghai University of Traditional Chinese Medicine,
No. 1200 Cailun Rd
Shanghai, China
E-mail: xjg@shutcm.edu.cn

Disclaimer: Drs. Ao-Lin Hou and Jia-Jia Wu contributed to the work equally. See pg. E155 for funding information.

Conflict of interest: Each author certifies that he or she, or a member of his or her immediate family, has no commercial association (i.e., consultancies, stock ownership, equity interest, patent/licensing arrangements, etc.) that might pose a conflict of interest in connection with the submitted manuscript.

Manuscript received: 07-17-2021
Revised manuscript received: 10-11-2021
Accepted for publication: 11-01-2021

Free full manuscript: www.painphysicianjournal.com

Background: Neuropathic pain following brachial plexus avulsion injury (BPAI) induces plastic changes in multiple brain regions associated with somatosensory function, pain, or cognition at the group level. The alternation of the whole pattern of resting-state brain activity and the feasibility of a brain imaging, information-based diagnosis of pain following BPAI is poorly investigated.

Objectives: To investigate whether brain pattern alternation can identify neuropathic pain from healthy controls at an individual level and the specific regions that can be used as diagnostic neuroimaging biomarkers.

Study Design: Controlled animal study.

Setting: The research took place in the school of rehabilitation science of a university and affiliated hospitals.

Methods: A total of 48 female Sprague-Dawley rats weighing 180 g–200 g were randomly assigned to either the BPAI group (n = 24) or normal control group (n = 24). A neuropathic pain rat model following BPAI was established in the BPAI group and a mechanical withdrawal threshold (MWT) test was performed to verify the presence of neuropathic pain. Micro-positron emission tomography with [Fluorine-18]-fluoro-2-deoxy-D-glucose (18F-FDG-PET) was used to obtain the whole brain metabolic activity scans. Multivariate pattern analysis (MVPA) was performed with a linear support vector machine (SVM) analysis both in PRoNTo toolbox (based on regions of interests) and SearchlightSearchlight approach (based on voxels within the region).

Results: Compared with baseline status, MWT of the left (intact) forepaw was significantly reduced in the BPAI group ($P < 0.001$). The accuracy of a whole brain image that correctly discriminated BPAI from normal controls rats was 87.5% with both the PRoNTo toolbox and SearchlightSearchlight method. Pearson's correlation analysis revealed significant positive correlations ($P < 0.05$) between MWT and the standard taken values of brain regions including the left olfactory nucleus, right entorhinal cortex in the PRoNTo toolbox, and bilateral amygdala, right piriform cortex and right ventral hippocampus in Searchlight method.

Limitations: The alternation of metabolic connectivity among regions and functional connectivity among different networks were not investigated in the present study.

Conclusions: Our study indicated that MVPA based on the PET scans of rats' brains could successfully identify neuropathic pain from health condition at the individual level and predictive regions could potentially be provided as neuroimaging biomarkers for the neuropathic pain following BPAI.

Key words: Neuropathic pain, brachial plexus avulsion injury, PET/CT, neuroimaging, multivariate pattern analysis, PRoNTo, SearchlightSearchlight, machine learning

Pain Physician 2022: 25:E147-E156

Brachial plexus avulsion injury (BPAI) is one of the most devastating peripheral nerve injuries in the upper extremity. Partial or global avulsion of C5, C6, C7, C8 and T1 nerve roots lead to sensory and motor dysfunction in the affected limb, which will obviously lower the quality of life in patients. Other than that, BPAI produces persistent and long-lasting painful behavior, which has been a widely concerned issue for many years. It is reported that 70%-90% of BPAI patients will develop neuropathic pain (1).

Many studies have suggested that central sensitization plays a critical role in the mechanism of neuropathic pain following BPAI. Ligation, crushing or avulsion injury of the brachial plexus induces nociceptive input signals to the central nervous system via several signal transmission pathways of pain, such as the spinothalamic pathway (2). Therefore, these nociceptive input signals induce persistently high reactions of neurons in associated pathways and alternation of neuroplasticity in several brain regions (2-4). The development of novel brain imaging techniques provides us the opportunity to investigate the central mechanism of neuropathic pain. Our previous studies based on functional magnetic resonance imaging (fMRI) also showed that neuropathic pain following BPAI induced plastic changes in multiple brain regions associated with somatosensory function, pain, or cognition at the group level (5).

Multivariate pattern analysis (MVPA) has been proposed as a powerful technique in investigating information coding in the brain. It is based on machine learning techniques to analyze distributed patterns of brain activity, which has more advantages than traditional univariate analysis (6). MVPA focuses on predicting a variable of interest from the pattern of brain activation/anatomy over a set of voxels or regions. Therefore, it has greater sensitivity and is capable of detecting subtle distinctions (7). MVPA has been used in distinguishing patients from healthy patients, including schizophrenia-spectrum disorder (8), Alzheimer disease (9), multiple sclerosis, and social anxiety disorder (10).

Based on our previous studies, BPAI could steadily induce long-lasting neuropathic pain in the affected limb of rats. It has also been demonstrated that neuropathic pain induces plastic changes in several brain regions (5,11,12). However, there has been no study focused on the alternation of the whole pattern of resting-state brain activity and the feasibility of brain imaging information-based diagnosis of pain following BPAI at the individual level. Therefore, we hypothesized BPAI could also alter the whole pattern of resting-state brain activity and the altered pattern of brain regions capable of identifying neuropathic pain in rats from healthy controls.

We established BPAI in rats and obtained whole brain metabolic activity by using micro-positron emission tomography with [Fluorine-18]-fluoro-2-deoxy-D-glucose (18F-FDG) positron emission tomography (PET). MVPA was applied to determine the brain regions that play important roles in identifying the brain with neuropathic pain following BPAI from that of control rats at the individual level. MVPA was performed with linear support vector machine (SVM) analysis both in the Pattern Recognition for Neuroimaging Toolbox (University College, London, United Kingdom) (PRoNTo) and SearchlightSearchlight approach. Prediction performance was evaluated by leave-one-out cross-validation (LOOCV). This outcome may provide novel insights to further understanding neuropathic pain following BPAI.

Methods

Animals and Surgery

A total of 48 female Sprague-Dawley rats weighing 180 g–200 g were provided by Shanghai Slack Laboratory Animal Limited Liability Company (Shanghai, China). They were raised under a 12 hour light/dark cycle with unrestricted food and water. Before any further intervention or assessment started, they were kept in cages for at least 7 days to acclimate them to their environment. The rats were randomly assigned to either a BPAI group (n = 24) or the normal control (NC) group (n = 24).

Neuropathic pain was induced by unilateral (right) brachial plexus avulsion injury as our previous studies reported (5,11). Briefly, the rat was anesthetized by intraperitoneal injection with sodium pentobarbital (40 mg/kg), and then placed in prone on a clean surgical table. A skin incision was made, and complex muscles were divided under an operative microscope (magnification ×10). The muscles on the vertebral plate and the spinous process were removed, and hemilaminectomies from C4 to T1 were performed to expose all the nerve roots of C5-T1 on the right side. All the right brachial plexus nerves were identified under direct vision. Both dorsal and ventral rootlets were grasped with forceps and completely extracted from the spinal cord by traction. A glutin sponge was applied for hemostasis, and the incisions were covered with penicillin powder to prevent infection.

Behavior Assessment

To confirm the successful induction and maintenance of neuropathic pain, all rats were tested for mechanical withdrawal threshold (MWT). MWT of the left (intact) forepaw was assessed in both groups (3 days pre-BPAI and on the 7th post-BPAI day) to evaluate the successful establishment of neuropathic pain. MWT was assessed by the method described previously by using a von Frey filament (13). Rats were placed on a metal mesh floor (0.8×0.8 cm^2 cells) covered by a transparent plastic box that was kept at 30 cm above the floor. After approximately 15 minutes of adaption, we fixed its hind limb with a nipper when the forepaw fell into the grid. The von Frey filament was used to apply a linearly increasing pressure on the forepaw until the rat withdrew it. The stimulating duration was 6 seconds-8 seconds, and the interval between stimulations was 30 seconds. The test was repeated 5 times, and the threshold was described as the lowest force that twice evoked a consistent brisk withdrawal response.

^{18}F-FDG-PET Image Acquisition

PET images of the brain were acquired 7 days after BPAI surgery. Images were acquired from a small animal PET/CT (computed tomography) scanner (Concorde Microsystems, Knoxville, TN).

In order to enhance 18F-FDG uptake in the brain, all 48 rats were deprived of food for 12 hours before PET/CT scans. 18F-FDG (0.5 mCi/100 g) was injected via the tail vein, and then the rats were placed in a quiet room for 30 minutes to ensure sufficient take up of the tracer. The rat was placed prone position on the bed of a PET/CT, which consisted of a 15-cm-diameter ring of 96 position sensitive ray scintillation detectors and provided a 10.8-cm trans-axial and a 7.8-cm axial field of view with an intrinsic resolution of 1.8 mm. The timing resolution was less than 1.5 nanoseconds. During scanning, an anesthesia dose of 5% halothane gas was administered for induction and 1.5% for maintenance. CT images were obtained for coregistration and attenuation correction. The collected images were reconstructed in the OSEM3D mode in a 128 × 128 matrix. The parameters of CT image acquisition were set as follows: spherical tube voltage = 80 kV, current = 500 μA, and acquisition time = 492 seconds.

Image preprocessing

Data preprocessing was conducted with Statistical Parametric Mapping 8 toolbox (SPM 8; http://www.fil.ion.ucl.ac.uk/spm/) based on Matlab 2014a (Mathworks, Inc., Natick, MA). Briefly, brain PET/CT images were obtained and then converted into the NIFTI format. The voxels were upscaled by ×10 times the original size. Then, the first image was chosen as a reference and the remaining volumes were realigned to generate an aligned set of images. Next, the aligned PET/CT images were normalized. The PET/CT images were reformatted into isotropic voxels (2 × 2 × 2 mm^3). The intensity was adjusted by the global mean. Finally, the images were smoothed by a full width at half maximum twice the voxel size.

Multivariate Pattern Analysis (MVPA)

MVPA with Pattern Recognition for Neuroimaging Toolbox (PRoNTo)

Linear SVM was employed as a classifier for machine learning and carried out with the PRoNTo toolbox, also based on Matlab 2014a (7). The BPAI and normal groups were entered as 2 classes with brain PET images as inputs. Both whole brain and BPAI-induced neuropathic pain related regions of interest (ROI) analyses were performed. ROIs included sensorimotor cortex (including bilateral somatosensory and motor cortices) and pain matrix (including bilateral anterior cingulate cortex [ACC], insular and thalamus) (14). LOOCV was performed as follows: in the n subjects (n = 48 in the present experiment) cross-validation, N-1 subjects were used as training data to train the linear classifier and the remaining sample was used for testing. The validation procedure was repeated 48 times and a different remaining subject was used for testing. Statistical significance of the classification was tested using a permutation test with 1,000 permutations.

MVPA with Searchlight and Principal Component Analysis (PCA) Method

As PRoNTo toolbox is based on ROIs, a modified MVPA method is based on all voxels within a region. The "SearchlightSearchlight and PCA" approach was applied to avoid overlooking any anatomical regions (15). It was performed to select an appropriate set of voxels to define multivariate features as the input of pattern classification analysis. In this approach, the smoothed brain PET images generated after the preprocessing procedure were the inputs of MVPA. We defined a small spherical cluster with a 4 mm radius which comprised 33 voxels of 2 mm width in each dimension for a given voxel Vi. Then the values of the clusters were extracted for each voxel in the fixed local cluster to yield a feature vector for voxel Vi. Feature matrix

W (N1*V) of training data set and W (N2*V) of testing data set were obtained. Then PCA was performed and the eigenvector was applied to the training data feature matrix to reduce the dimensionality, and then the data were used to train the classifier. Meanwhile, the eigenvector was also applied to the testing data feature matrix. Finally, the classification was performed with the SVM using LibSVM software (National Taiwan University, Taipei, Taiwan) (http://www. csie.ntu.edu.tw/cjlin/libsvm) (16).

The performance of the linear SVM classifier was also evaluated using LOOCV. Therefore, classifier accuracy for Vi was obtained by averaging the accuracies achieved for every subject cross-validation procedure. This procedure was performed for all voxels to obtain a 3-dimension map of classification accuracy at every voxel that discriminated between BPAI and normal rats. The permutation test was performed to evaluate the statistical significance of each voxel and the permutation was repeated 1,000 times. Then classification accuracies were thresholded by $P < 0.05$. The extent was thresholded as 100 voxels and classification accuracy was thresholded as 85% (10).

Correlation Analysis

To investigate the most important brain regions that discriminate between BPAI and NC were correlated with the severity of neuropathic pain, Pearson correlation analysis was applied between the accuracy of each voxel in the discriminative brain regions and the MWT of the intact forepaw based on the pooled BPAI and NC rats.

Study Approval

All procedures were in agreement with the Guide for the Care and Use of Laboratory Animals described by the US National Institutes of Health and were approved by the Animal Ethical Committee of Shanghai University of Traditional Chinese Medicine (approval number: SZY20171211001).

Results

Confirmation of Neuropathic Pain

The MWT of the left (intact) forepaw was 10.04 ± 1.31 g and 4.2 5± 1.33 g in the BPAI group 3 days pre-BPAI and 7th post-BPAI day, respectively and 9.79 ± 1.47g, and 9.58 ± 0.99 g similarly in the NC group. Compared with baseline status, the MWT significantly was reduced in the BPAI group ($P < 0.001$). No significant changes were found between pre-BPAI and post-BPAI in the NC group. Three of the 24 BPAI rats (12.5%) showed autotomic behavior in the right (injured side) forepaws, such as biting of the nails and digits. No severe autotomic behavior was observed.

MVPA with PRoNTo Toolbox

With SVM analyses of the 18F-FDG PET brain images, a significant balanced accuracy (BA) of 87.50% was obtained for classification of BPAI and normal rats when using the binary mask of whole brain ($P = 0.001$). The classification accuracy (CA) for BPAI rats was up to 95.83% ($P = 0.001$) while for normal rats it was 79.17% ($P = 0.003$). The area under the curve (AUC) of the receiver operating characteristic curve was 0.89.

Using information from grey matter, white matter, the pain matrix, the sensorimotor cortex, and the thalamus, the BAs in discriminating BPAI from NC were 87.50%, 87.50%, 87.50%, 87.50% and 83.33%, respectively (Table 1). The CAs and AUCs for each brain region are all included in Table 1. Several brain regions show greater weights than others. One standard deviation (0.87) greater than the average weight (1.05) of all regions was considered significant (10). Brain regions showing significantly greater weights include bilateral entorhinal cortex (EC), mesencephalic region (MR) and olfactory nuclei (ON). (Fig. 1).

MVPA with Searchlight + Principal Component Analysis Analysis

The accuracy of the whole brain image that correctly discriminated BPAI from NC rats was also 87.50% while applying Searchlight analysis. There were several areas presenting significant differences between BPAI and NC groups; the brain regions with accuracies of 85% or higher and cluster sizes of 100 or more are shown in Fig. 2 and Table 2.

Correlation Analysis

In order to investigate the correlation between the most discriminating brain regions and the severity of neuropathic pain, Pearson's correlation analysis results are shown in Fig. 3. For the discriminating brain regions in the PRoNTo analysis, the SUVs in the ROIs of the left olfactory nucleus (ON, r = 0.416) and right entorhinal cortex (EC, r = 0.4153) were positively correlated with the MWT. For the discriminating brain regions in the Searchlight and PCA analysis, the SUVs in the regions of the bilateral amygdala (left, r = 0.4355; right, r = 0.4079), right piriform cortex (PC, r = 0.4409) and right

Table 1. *Predictions of neuropathic pain induced by BPAI. The balanced accuracy, classification accuracies and AUC of ROC.*

Brain area	BA (p value)	CA for BPAI (p value)	CA for NC (p value)	AUC
Whole brain	87.50% (0.001)	95.83% (0.001)	79.17% (0.003)	0.89
Grey matter	87.50% (0.001)	95.83% (0.001)	79.17% (0.003)	0.86
White matter	87.50% (0.001)	95.83% (0.001)	79.17% (0.005)	0.88
Pain matrix	87.50% (0.001)	95.83% (0.001)	79.17% (0.004)	0.86
Sensorimotor cortex	87.50% (0.001)	95.83% (0.001)	79.17% (0.004)	0.85
Thalamus	83.33% (0.001)	91.67% (0.001)	75.00% (0.043)	0.85

BPAI: brachial plexus avulsion injury; NC: normal control; AUC: area under curve; ROC: receiver operating characteristic curve; BA: balanced accuracy; CA: classification accuracy.

ventral hippocampus (VH, r = 0.4078) were also positively correlated with the MWT.

Discussion

Chronic neuropathic pain has been a frequent concern in clinical practice. It is caused by lesion or disease of the central nervous system or/and peripheral nervous system such as stroke, postherpetic neuralgia, spinal cord injury, and traumatic nerve injury (17). The mechanism of neuropathic pain is complex, as both the peripheral and central nervous systems are involved (18). In order to simulate pain conditions, many surgical models, including spinal nerve ligation, spared nerve injury sciatic nerve trisection, and BPAI were developed and investigated (19,20).

The present study demonstrates neuropathic pain following BPAI altered resting-state brain metabolic pattern; MVPA using 18F-FDG PET could potentially distinguish rats with neuropathic pain following BPAI from normal rats with high classification accuracy. The current study is the first to apply MVPA to discriminate an animal model with neuropathic pain following BPAI from normal rats. Our study demonstrated 3 main findings: 1) By both PRoNTo and Searchlight analysis, the classification accuracies for neuropathic pain following BPAI were both 87.50% and the AUC value of PRoNTo analysis was 0.89. It indicated the diagnostic potential of the altered metabolic brain pattern. 2) Neuropathic pain following BPAI induced the changes of SUVs in several brain regions and activity pattern alteration could be selected as a classifier feature. 3) Some important brain regions could potentially provide neuroimaging biomarkers for neuropathic pain in BPAI rats.

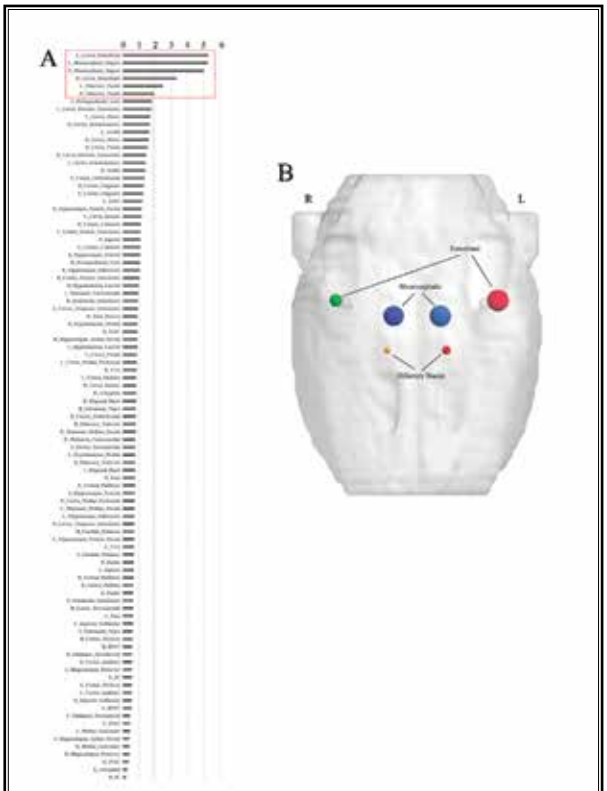

Fig. 1. *The region weight in the classification of BPAI and NC.*
(A) *Weights for the brain regions in descending order. The bars of red color indicate significantly higher weight (weight > 1.93).* (B) *Brain regions with significantly higher weight in the classification. The size of node represents the value of weight of the brain region.*
BPAI: brachial plexus avulsion injury; NC: normal control.

Neuropathic pain after BPAI is one of the deafferentation pains that share some similar symptoms reported in amputees (21-23). BPAI is a common clinical problem that often results from traffic accidents, and the incidence of persistent pain following this kind of injury is quite high (24). Compared with other diseases that cause neuropathic pain, studies focused on the mechanisms of BPAI are fewer. The rapid development of neuroimaging techniques, such as fMRI and PET/CT, helped us to explore its central mechanisms. It has been widely accepted that the pain experience results from a 3-dimensional integration of sensory-discriminative, affective-motivational, and cognitive-evaluative axes in which several brain regions are involved (25). It is extremely important to know that BPAI-induced neu-

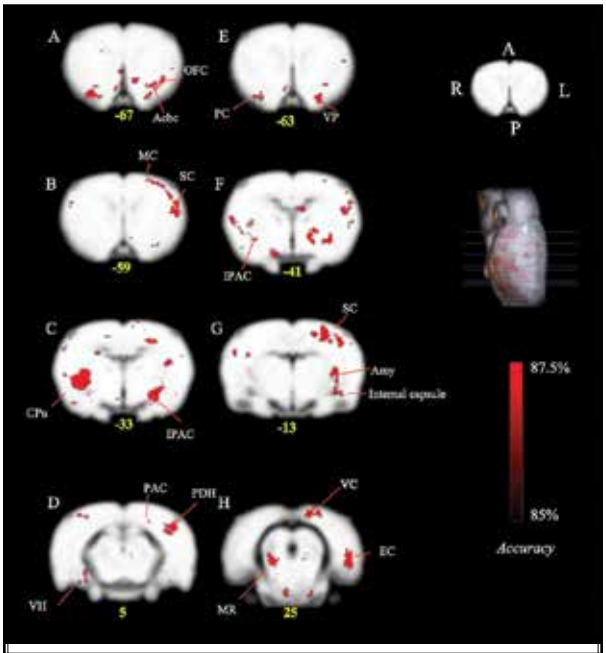

Fig. 2. *The spatial distribution of accuracy map for discriminating between BPAI and NC groups. Red clusters represent accuracy of 85% or higher with threshold cluster size of 100 voxels or more.*
BPAI: brachial plexus avulsion injury; NC: normal control; A: anterior; P: posterior; R: right; L: left; OFC: orbitofrontal cortex; Acbc: : PC: piriform cortex; VP: ventral pallidum; MC: motor cortex; SC: somatosensory cortex; IPAC: interstitial nucleus of the posterior limb of the anterior commissure; CPu: caudate putamen; Amy: amygdala; PAC: parietal association cortex; PDH: posterodorsal hippocampus; VH: ventral hippocampus; MR: mesencephalic region; VC: visual cortex; EC: entorhinal cortex.

roplasticity in several brain regions are associated with the occurrence and maintenance of chronic pain as well as the absence of sensorimotor function. Based on previous studies, there are brain regions responsible for sensorimotor function, including the somatosensory cortex, the primary motor cortex, the supplementary motor area and caudate putamen, and pain-related areas (26). It is suggested that the primary sensory cortex (S1), the secondary sensory cortex (S2), the insula, the ACC, the thalamus, and the prefrontal cortex, which constitute the pain matrix in the brain, are involved in the neuropathic pain (27). The view of pain matrix also suggested that pain is multidimensional and produced by distributed neural patterns (28). Our previous studies investigated neuropathic pain among resting-state, block-design brain activity and neural metabolism studies. Electrical stimulation on the forelimb induced decreased activation in the limbic/paralimbic system and somatosensory cortex (5). The changes in the amplitude of low frequency fluctuations is also found in several brain regions involving sensory, cognitive, and memory functions (5). The changes in brain metabolism also support the previous findings (11,12,29).

As for pain, few adequate biomarkers were widely used in clinical practice (30). It is acknowledged that pain is multidimensional, involving physical, psychological, emotional, cognitive and social aspects (31). Previous studies have demonstrated that neuropathic pain following the injury of the peripheral nervous system or central nervous system, is maintained by sensitization of an array of nervous system pathways, from spinal sensitization to cerebral sensitization (32,33).

The development of neuroimaging techniques helps us to investigate multiple brain features, which could potentially be used as biomarkers to predict the incidence or intensity of chronic pain (34). Marquand et al (35) predicted heat pain intensity using Gaussian process regression from whole-brain fMRI volumes. Callan et al (36) classified patients with chronic low back pain versus healthy patients with fMRI during evoked electrical stimulation on the back; their accuracy rate was 92.3%. Cheng et al (37) used regional blood oxygen level dependent signal variability/amplitude of low-frequency oscillations (LFOs) to identify functional brain abnormalities in patients with chronic pain that are related to chronic pain characteristics. They found that the abnormalities of LFOs, in particular within higher frequencies can be used to make generalizable inferences about trait neuropathic pain (average pain over the previous week) but not state pain (current pain) (37). Our finding could also be used to monitor the intensity of pain, although further validation still needs to be investigated.

Generally, univariate approaches based on neuroimaging techniques, could analyze each voxel or average across voxels' signals in a region, which have limitations to the researches. More recently, MVPA has become a feasible technique in the analysis of neuroimaging, which could analyze distributed patterns of brain activity or anatomy using machine learning classifiers (38,39). It has been widely used in several studies ranging from decoding mental states to clinical applications (10,40-44). For example, Polyn et al (45) applied MVPA to predict the patterns of cortical activity associated with memory search during free recall tasks. MVPA with fMRI also allows the decoding of patterns of brain response in different categories of the viewed objects (40,46). Moreover, the capacity of discriminating control and experimental groups has been

Table 2. *The most important brain regions discriminating BPAI and NC groups in searchlight + PCA method.*

Brain regions	Peak accuracy (%)	Cluster size (voxels)	MNI coordinates (mm)			*p* value
			x	y	z	
Right amygdala	87.50	707	42	-30	-19	0.001
Right piriform cortex	87.50	707	61	-38	-21	0.001
Left somatosensory cortex	87.50	567	-54	3	-61	0.001
Left amygdala	87.50	514	-44	-32	-13	0.001
Left IPAC	87.50	514	-42	-26	-33	0.001
Left visual cortex	87.50	295	-54	24	9	0.001
Left parietal association cortex	87.50	242	-34	28	-3	0.001
Left entorhinal cortex	87.50	177	-57	-22	29	0.001
Left ventral pallidum	87.50	175	-28	-40	-63	0.001
Left orbitofrontal cortex	87.50	175	-38	-17	-67	0.001
Right ventral hippocampus	87.50	123	40	-38	5	0.001
Left posterodorsal hippocampus	85.42	295	-57	3	3	0.001
Right caudate putamen	85.42	707	44	-11	-27	0.001
Left AcbC	85.42	175	-18	-26	-73	0.001
Left internal capsule	85.42	514	-46	-11	-11	0.001
Left motor cortex	85.42	567	-27	34	-58	0.001
Right IPAC	85.42	707	38	-27	-39	0.001

BPAI: brachial plexus avulsion injury; NC: normal control; PCA: principal component analysis; MNI: Montreal Neurological Institute; Acbc: nucleus accumbens-core; IPAC: interstitial nucleus of the posterior limb of the anterior commissure

proven in many clinical conditions, which suggests that MVPA can potentially be used as a diagnostic tool (47). Feng (10) suggested that the classification accuracy of patients into healthy and social anxiety disorder patients, using functional connectivity MRI, achieved 82.5% (10). Christian (48) suggested that multivariate analysis showed superior diagnostic performance with high classification accuracy in discriminating healthy patients and patients with Alzheimer disease rather than univariate analysis. MVPA with linear SVM also successfully identified the brain with neuropathic pain following spinal nerve ligation in an individual rat model using 18F-FDG PET (49).

The present study shows that MVPA achieved high classification accuracy using both PRoNTo and Searchlight analysis. Although the involved brain regions in the 2 analyses differed, these regions were mostly consistent with previous studies. In the PRoNTo analysis, bilateral EC, MR, and ON showed significantly greater weights; the left EC had the highest weight. In Searchlight analysis, the regions that had the highest accuracy included the right amygdala, right PC, right VH, left somatosensory cortex (SC), left interstitial nucleus of the posterior limb of the anterior commissure (IPAC), left visual cortex (VC), left parietal association cortex (PAC), left EC, left ventral pallidum (VP) and left orbitofrontal cortex (OFC). Prefrontal-limbic-brainstem, olfactory, visual and sensory networks were involved, which indicated the multidimensional characteristics of pain perception and distributed representation in the brain. Pearson correlation analysis showed that the SUVs of the left ON, right EC, bilateral Amygdala, right PC and right VH were positively correlated with the MWT.

ON and PC constituted part of the primary olfactory cortex. Previous studies have focused on the PC; far fewer have examined ON and the olfactory bulb. PC was considered associating with encoding information about the chemical attributes of odorants and perceptual quality of odors in previous studies (50-52). ON may be involved in odor memory and localization, which allows PC to perform more associative functions (53,54). Zhou et al (55) have suggested that PC has strong functional connectivity with motor planning areas, including the caudate/putamen and the primary motor cortex, which indicated that PC may be involved in combining olfactory information with motor planning (55). In addition, studies also found that the temporal piriform cortex was connected to the brainstem raphe magnus and posterior insula in humans, areas implicated in pain processing (56) and respiratory modulations (57).

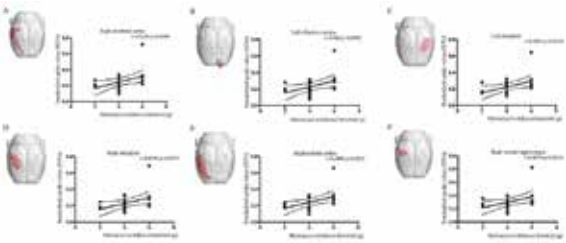

Fig. 3. *Correlation between the SUVs of brain regions of interest and the MWT of the intact forepaw based on the post-BPAI data.*
(A) *Map of brain area of the right EC. A positive correlation was found between the SUVs in ROIs of right EC and MWT (r = 0.4153, p = 0.0436).* (B) *Map of brain area of the left ON. A positive correlation was found between the SUVs in ROIs of left ON and MWT (r = 0.416, p = 0.0432).* (C) *Map of brain area of the left amygdala. A positive correlation was found between the SUVs in ROIs of left amygdala and MWT (r = 0.4355, p = 0.0334).* (D) *Map of brain area of the right amygdala. A positive correlation was found between the SUVs in ROIs of right amygdala and MWT (r = 0.4079, p = 0.0479).* (E) *Map of brain area of the right PC. A positive correlation was found between the SUVs in ROIs of right PC and WMT (r = 0.4409, p = 0.0311).* (F) *Map of brain area of the right VH. A positive correlation was found between the SUVs in ROIs of right VH and MWT (r = 0.4078, p = 0.0479).*
BPAI: brachial plexus avulsion injury; ROIs: regions of interest; SUVs: standardized uptake values; MWT: mechanical withdrawal threshold; ON: olfactory nuclei; EC: entorhinal cortex; PC: piriform cortex; VH: ventral hippocampus.

EC and the hippocampus belong to the limbic system, which is considered to be involved in emotional processing and providing relevant and motivational information for complex behaviors regulation (58). EC has long been considered as a main station that provides pain signals and other afferent input to the hippocampus (59). Although the exact pathway between EC and the hippocampus formation is still unclear, the Papez circuit and cortico-limbic pathway might play an important role in it. The Papez circuit, proposed by James Papez in 1937, includes the hippocampus subiculum, fornix, mammillary bodies, mammillothalamic tract, anterior thalamic nucleus, cingulum, and EC, and finally comes back to hippocampus formation (HF) (60,61). The circuit showed that some pain-related regions were connected with EC and HF, such as the ACC. The cortico-limbic pathway was from the primary and secondary somatosensory cortices to insular and parietal cortical structures, then to the amygdala, the perirhinal cortex and the hippocampus, and finally projects to regions that were directly activated by the spinothalamic pathways (62,63). In the cortico-limbic pathway, EC might receive pain signal input from the insular and convey it to HF (63,64). Our previous study also suggested that the entorhinal-hippocampus pathway might play an important role in persistent peripheral pain processing of BPAI (5).

The amygdala also belongs to the limbic system, which is involved in emotions and affective disorders (65,66). It has been widely accepted that the amygdala might be a critical node in the emotional affective aspects of pain (67,68). It has extensive afferent and efferent connections with multiple cortical and subcortical regions (69). It receives excitatory inputs from visual, auditory, somatosensory (pain), olfactory, and taste systems and projects to the hypothalamus, bed nucleus of the terminalis, midbrain periaqueductal gray, pons, medulla, prefrontal cortex, olfactory cortex, and brain stem (70). The connectivity between the olfactory cortex and amygdala also suggest that the olfactory cortex might play a role in the processing of emotion.

Our experiment has some limitations. First, the natural differences between humans and rodents should not be neglected. Further studies in patients with BPAI still need to be investigated. Secondly, although our study provides notable information about the regions that represent the alternation of neuropathic pain following BPAI, it is not clear how the regions change the inter-connectivity. Lastly, our study indicates that altered regions are involved with several networks; the changes among different networks such as default mode network still need further investigation.

Conclusion

Our study demonstrates that multivariate pattern analysis based on PET scans of rats' brains can successfully discriminate neuropathic pain following BPAI from the health condition on an individual level. Both of the 2 approaches, which are based on ROIs or whole voxel of brain regions, showed significant discriminative performance. Alternation of the pattern of brain resting-state activity could potentially be used as a diagnostic tool in the future.

Authorship Contributions

Ao-Lin Hou monitored collection and analysis of data and written the manuscript. Xiang-Xin and Jia-Jia Wu analyzed the data and made revision of the method section. Bei-Bei Huo and Jun Shen designed the study and monitored the progress and data collec-

tion. Mou-Xiong Zheng and Xu-Yun Hua analyzed and interpreted the data and made critical revision of the paper. Mou-Xiong Zheng, Xu-Yun Hua, Jian-Guang Xu supervised the progress of the study.

Funding

National Key R&D Program of China (Grant No.: 2018YFC2001600); National Natural Science Foundation of China (Grant Nos.: 81802249 and 81871836); Shanghai Science and Technology Committee (Grant Nos.: 18511108300, 18441903900 and 18441903800); Shanghai Rising-Star Program (Grant No.: 19QA1409000); Shanghai Municipal Commission of Health and Family Planning (Grant No.: 2018YQ02 and 201840224); Shanghai Youth Top Talent Development Plan and Shanghai "Rising Stars of Medical Talent" Youth Development Program (Grant No.: RY411.19.01.10) and Shanghai Youth Top-notch Talent Program.

References

1. Teixeira MJ, da Paz MG, Bina MT, et al. Neuropathic pain after brachial plexus avulsion--central and peripheral mechanisms. *BMC Neurol* 2015; 15:73.
2. Crofford LJ. Chronic pain: Where the body meets the brain. *Trans Am Clin Climatol Assoc* 2015; 126:167-183.
3. Latremoliere A, Woolf CJ. Central sensitization: A generator of pain hypersensitivity by central neural plasticity. *J Pain* 2009; 10:895-926.
4. Jaggi AS, Singh N. Role of different brain areas in peripheral nerve injury-induced neuropathic pain. *Brain Res* 2011; 1381:187-201.
5. Wang S, Ma ZZ, Lu YC, et al. The localization research of brain plasticity changes after brachial plexus pain: Sensory regions or cognitive regions? *Neural Plast* 2019; 2019:7381609.
6. Pereira F, Mitchell T, Botvinick M. Machine learning classifiers and fMRI: A tutorial overview. *Neuroimage* 2009; 45:S199-S209.
7. Schrouff J, Rosa MJ, Rondina JM, et al. PRoNTo: Pattern Recognition for neuroimaging toolbox. *Neuroinformatics* 2013:11;319-337.
8. Mikolas P, Hlinka J, Skoch A, et al. Machine learning classification of first-episode schizophrenia spectrum disorders and controls using whole brain white matter fractional anisotropy. *BMC psychiatry* 2018; 18: 97.
9. Vemuri P, Gunter JL, Senjem ML, et al. Alzheimer's disease diagnosis in individual subjects using structural MR images: Validation studies. *Neuroimage* 2008: 39;1186-1197.
10. Liu F, Guo W, Fouche JP, et al. Multivariate classification of social anxiety disorder using whole brain functional connectivity. *Brain Structure & Function* 2015; 220:101-115.
11. Shen J, Huo BB, Zheng MX, et al. Evaluation of neuropathic pain in a rat model of total brachial plexus avulsion from behavior to brain metabolism. *Pain Physician* 2019; 22:E215-E224.
12. Shen J, Huo BB, Hua XY, et al. Cerebral 18 F-FDG metabolism alteration in a neuropathic pain model following brachial plexus avulsion: A PET/CT study in rats. *Brain Research* 2019; 1712.
13. Rodrigues-Filho R, Santos AR, Bertelli JA, et al. Avulsion injury of the rat brachial plexus triggers hyperalgesia and allodynia in the hindpaws: A new model for the study of neuropathic pain. *Brain Res* 2003; 982:186-194.
14. Iannetti GD, Mouraux A. From the neuromatrix to the pain matrix (and back). *Experimental Brain Research* 2010; 205:1-12.
15. Min, Xu, Daniel, et al. Distinct distributed patterns of neural activity are associated with two languages in the bilingual brain. *Science advances* 2017.
16. Oosterhof NN, Connolly AC, Haxby JV. CoSMoMVPA: Multi-modal multivariate pattern analysis of neuroimaging data in Matlab/GNU octave. *Frontiers in Neuroinformatics* 2016; 10.
17. Zilliox LA. Neuropathic Pain. *Continuum Lifelong Learning in Neurology* 2017; 23:512-532.
18. Cohen SP, Mao J. Neuropathic pain: Mechanisms and their clinical implications. *BMJ* 2014; 348:f7656.
19. Challa SR. Surgical animal models of neuropathic pain: Pros and Cons. *Int J Neurosci* 2015; 125:170-174.
20. Vierck CJ, Hansson PT, Yezierski RP. Clinical and pre-clinical pain assessment: are we measuring the same thing? *Pain* 2008; 135:7-10.
21. David B, Abdel-Maguid TE. Superficial dorsal horn of the adult human spinal cord. *Neurosurgery* 1984; 893.
22. Lamotte C. Distribution of the tract of Lissauer and the dorsal root fibers in the primate spinal cord. *Journal of Comparative Neurology* 1977; 172:529.
23. Light, Alan R. Normal Anatomy and Physiology of the Spinal Cord Dorsal Horn. *Applied Neurophysiology* 1988; 51:78-88.
24. Umansky D, Midha R. Treatment of neuropathic pain after peripheral nerve and brachial plexus traumatic injury. *Neurol India* 2019; 67:S23-S24.
25. Melzack R, Casey KL. *Sensory, Motivational, and Central Control Determinants of Pain*, 1968.
26. Feng JT, Liu HQ, Hua XY, et al. Brain functional network abnormality extends beyond the sensorimotor network in brachial plexus injury patients. *Brain Imaging & Behavior* 2015; 10:1-8.
27. Davis KD, Flor H, Greely HT, et al. Brain imaging tests for chronic pain: medical, legal and ethical issues and recommendations. *Nature Reviews Neurology* 2017.
28. Garcia-Larrea L, Peyron R. Pain matrices and neuropathic pain matrices: A review. *Pain* 2013; 154:S29-S43.
29. Huo BB, Shen J, Hua XY, et al. Alteration of metabolic connectivity in a rat model of deafferentation pain: A 18F-FDG PET/CT study. *J Neurosurg* 2019; 1-9.
30. Woo CW, Chang LJ, Lindquist MA, et al. Building better biomarkers: Brain models in translational neuroimaging. *Nature Neuroscience* 2017; 20:365-377.
31. Carlino E, Frisaldi E, Benedetti F. Pain and the context. *Nature Reviews Rheumatology* 2014; 10:348-355.
32. Teixeira MJ, Paz MGDSD, Bina MT, et al. Neuropathic pain after brachial plexus avulsion - central and peripheral mechanisms. *Bmc Neurology* 2015; 15:1-9.
33. Kuner R, Flor H. Structural plasticity and reorganisation in chronic pain. *Nature Reviews Neuroscience* 2016; 18:113.
34. Van D, Lindquist MA, Wager TD.

Neuroimaging-based biomarkers for pain: State of the field and current directions. *PAIN Reports* 2019; 4.

35. A AM, A MH, B MB, et al. Quantitative prediction of subjective pain intensity from whole-brain fMRI data using Gaussian processes. *NeuroImage* 2010; 49:2178-2189.
36. Daniel C, Lloyd M, Connie N, et al. A tool for classifying individuals with chronic back pain: Using Multivariate Pattern Analysis with Functional Magnetic Resonance Imaging Data. *Plos One* 2014:9: e98007.
37. Rogachov, Anton, Cheng, et al. Abnormal low-frequency oscillations reflect trait-like pain ratings in chronic pain patients revealed through a machine learning approach. *Journal of Neuroscience the Official Journal of the Society for Neuroscience* 2018.
38. Woolgar A, Jackson J, Duncan J. Coding of visual, auditory, rule, and response information in the brain: 10 Years of multivoxel pattern analysis. *Journal of Cognitive Neuroscience* 2016; 28:1433-1454.
39. Cox DD, Savoy RL. Functional magnetic resonance imaging (fMRI) "brain reading": Detecting and classifying distributed patterns of fMRI activity in human visual cortex. *NeuroImage* 2003; 19:261-270.
40. Haxby JV, Gobbini MI, Furey ML, et al. Distinct, overlapping representations of faces and multiple categories of objects in ventral temporal cortex. *NeuroImage* 2001.
41. Lee YS, Janata P, Frost C, et al. Investigation of melodic contour processing in the brain using multivariate pattern-based fMRI. *Neuroimage* 2011; 57:293-300.
42. Ecker C, Rocha-Rego V, Johnston P, et al. Investigating the predictive value of whole-brain structural MR scans in autism: A pattern classification approach. *Neuroimage* 2010; 49:44-56.
43. Sapountzis P, Schluppeck D, Bowtell R, et al. A comparison of fMRI adaptation and multivariate pattern classification analysis in visual cortex. *Neuroimage* 2010; 49:1632-1640.
44. Spiridon M, Kanwisher N. How distributed is visual category information in human occipito-temporal cortex? An fMRI study. *Neuron* 2002; 35:1157-1165.
45. Polyn SM, Natu VS, Cohen JD, et al. Category-specific cortical activity precedes retrieval memory search. *Science* 2006; 310:1963-1966.
46. Chaimow D, Yacoub E, Ugurbil K, et al. Modeling and analysis of mechanisms underlying fMRI-based decoding of information conveyed in cortical columns. *Neuroimage* 2011; 56:627-642.
47. Kloppel S, Abdulkadir A, Jack CR, et al. Diagnostic neuroimaging across diseases. *Neuroimage* 2012; 61:457-463.
48. Habeck C, Foster NL, Perneczky R, et al. Multivariate and univariate neuroimaging biomarkers of Alzheimer's disease. *Neuroimage* 2008; 40:1503-1515.
49. Kim CE, Yu KK, Chung G, et al. Identifying neuropathic pain using 18 F-FDG micro-PET: A multivariate pattern analysis. *Neuroimage* 2014; 86:311-316.
50. Bensafi M, Sobel N, Khan RM. Hedonic-specific activity in piriform cortex during odor imagery mimics that during odor perception. *Journal of Neurophysiology* 2007; 98:3254-3262.
51. Zelano C, Bensafi M, Porter J, et al. Attentional modulation in human primary olfactory cortex. *Nature Neuroscience* 2005; 8:114-120.
52. Schulze P, Bestgen AK, Lech RK, et al. Preprocessing of emotional visual information in the human piriform cortex. *Scientific Reports* 2017; 7:9191.
53. Aqrabawi AJ, Chul KJ. Hippocampal projections to the anterior olfactory nucleus differentially convey spatiotemporal information during episodic odour memory. *Nature Communications* 2018; 9:2735-.
54. Kikuta S, Sato K, Kashiwadani H, et al. Neurons in the anterior olfactory nucleus pars externa detect right or left localization of odor sources. *Proceedings of the National Academy of Sciences* 2010; 107:12363-12368.
55. Zhou G, Lane G, Cooper SL, et al. Characterizing functional pathways of the human olfactory system. *eLife Sciences* 2019; 8.
56. Woo MA, Kumar R, Macey PM, et al. Brain injury in autonomic, emotional, and cognitive regulatory areas in patients with heart failure. *Journal of Cardiac Failure* 2009; 15:214-223.
57. Evans KC, Dougherty DD, Schmid AM, et al. Modulation of spontaneous breathing via limbic/paralimbic-bulbar circuitry: An event-related fMRI study. *Neuroimage* 2009; 47:961-971.
58. Morgane PJ, Galler JR, Mokler DJ. A review of systems and networks of the limbic forebrain/limbic midbrain. *Progress in Neurobiology* 2005; 75:143-160.
59. Van Strien NM, Cappaert NLM, Witter MP. The anatomy of memory: an interactive overview of the parahippocampal-hippocampal network. *Nature Reviews Neuroscience* 2009; 10:272-282.
60. Papez JWM. A Proposed mechanism of emotion. *Archneurolpsychiat* 1937; 38:103-112.
61. Abhidha, Shah, and, et al. Analysis of the anatomy of the Papez circuit and adjoining limbic system by fiber dissection techniques. *Journal of Clinical Neuroscience* 2012.
62. Vaccarino AL, Melzack R. Temporal processes of formalin pain: differential role of the cingulum bundle, fornix pathway and medial bulboreticular formation. *Pain* 1992; 49:257-271.
63. Friedman DP, Murray EA, O'Neill JB, et al. Cortical connections of the somatosensory fields of the lateral sulcus of macaques: Evidence for a corticolimbic pathway for touch. *Journal of Comparative Neurology* 1986; 252:323-347.
64. Mesulam MM, Mufson EJ. Insula of the old world monkey. III: Efferent cortical output and comments on function. *Journal of Comparative Neurology* 1982; 212:38-52.
65. Elman I, Borsook D. Common brain mechanisms of chronic pain and addiction. *Neuron* 2016; 89:11-36.
66. Neugebauer V. Amygdala pain mechanisms. *Handb Exp Pharmacol* 2015; 227:261-284.
67. Simons LE, Moulton EA, Linnman C, et al. The human amygdala and pain: Evidence from neuroimaging. *Human Brain Mapping* 2014; 35.
68. Thompson JM, Neugebauer V. Cortico-limbic pain mechanisms. *Neuroscience Letters* 2018.
69. PITKÄNEN A, Pikkarainen M, Nurminen N, et al. Reciprocal connections between the amygdala and the hippocampal formation, perirhinal cortex, and postrhinal cortex in rat. A review. *Ann N Y Acad* 2010; 911:369-391.
70. Roy AK, Shehzad Z, Margulies DS, et al. Functional connectivity of the human amygdala using resting state fMRI. *Neuroimage* 2009; 45:614-626.